CIENTIFIC Publishing Limited

Prevention and Treatment of Natural Disasters
http://ojs.ukscip.com/index.php/ptnd

ARTICLE

Volcanism and Curie Isotherm Distribution in the Jalisco Block, Mexico

Vladimir Palafox[1] Román Alvarez[2*]

1. Engineering Department, National University of Mexico, Mexico
2. Research Institute of Applied Mathematics and Systems (IIMAS), National University of Mexico, Mexico

Received: 25 February 2022; **Accepted:** 5 May 2022; **Published Online:** 24 May 2022

Abstract: A suitable combination of magnetic field determinations is assembled in the whole area of the Jalisco block in central-western Mexico; it serves as the basis for calculations of the Curie Point Isotherm by means of Spectral Analysis. The Jalisco block contains numerous volcanic manifestations; an attempt is made at correlating the Curie Isotherm (CI) with volcanic manifestations and its implicit risk to nearby populated regions. A preliminary analysis of this isotherm is carried out using areas of 60 × 60 km^2, where the volcanic regions at the NW and SE portions of the Tepic-Zacoalco (T-Z) rift coincide with shallow layers of the CI. Results show an unexpected region in the middle of the T-Z rift, where the isotherm deepens to 12 km depth and volcanism appears to be missing. The authors argue that this phenomenon may be associated with a flare up episode occurring at 5-3 Ma along the rift. Varying the area used for the calculation of the CI, from 30 × 30 km^2 to 120 × 120 km^2, illustrateshow the concomitant changes in volume affect the depth of penetration. The authors find exceptional regions in which the CI shows shallow depths at all area sizes used in the calculations; this consistency is interpreted as a magnetic alteration of the crust originating at mid-crustal depths. These regions also correspond to high values of the Bouguer anomaly reported elsewhere. Six magneto-stratigraphic profiles are presented for the results of the 60 × 60 km^2 calculations, where geologic, topographic, and magnetic properties are displayed along their length.

Keywords: Spectral analysis; Total magnetic field; Aeromagnetic data; Rift; Flare-up; Volcanic risk; Magneto-strati- graphic profiles

1. Introduction

The Jalisco block (JB), in central western Mexico, is described as a tectonic unit, an incipient microplate, whose extent has been largely defined by the capture of Baja California peninsula by the Pacific plate [1-4]. It is bounded to the NW by the Extensional Gulf Province, to the N by the Sierra Madre Occidental, and to the SE by the Michoacán block. The NW portion of the Trans-Mexican Volcanic Belt (TMVB) overlaps some regions of the

*Corresponding Author:
RománAlvarez,
Research Institute of Applied Mathematics and Systems (IIMAS), National University of Mexico, Mexico;
Email: Roman.alvarez@iimas.unam.mx

DOI: https://doi.org/10.54963/ptnd.v1i1.37

JB (Figure 1). Two rifts flank the JB, to the N it is bounded by the Tepic-Zacoalco rift [2], and to the E by the Colima rift [1]. A third rift closing the NW limit of the JB has been proposed [5], disclosing the presence of a triple point (rift-rift-rift) along the Tepic-Zacoalco (T-Z) rift, referred to as the Compostela triple point. With this third branch the JB is fully delimited by rift structures on the continental portion.

From the topographic viewpoint the JB is clearly divided into two segments: a region of low elevations extending from the coast to ~70 km inland and, continuing inland, a region of elevations varying between 1200 m to 2200 m; Alvarez et al. [6] referred to these two regions as the static and the uplifted domains of the JB, respectively. Given several similarities, the model for uplift proposed by Cassel et al. [7] illustrates a viable mechanism by which elevation of the JB might have occurred. Volcanism in the uplifted region is common, whilst in the static domain it is absent [8]. An association of volcanism and gravity involving the whole JB shows that volcanic fields present negative Bouguer anomalies exhibiting several correlations in that area [5]. Since the present study also encompasses the whole JB, in the section of Conclusions we correlate two main gravimetric regions of the JB with results of the Curie Isotherm reported here.

Volcanism in the JB encompasses rhyolitic ash-flow tuffs from 92 Ma to 65 Ma [9,10] to Pliocene-Quaternary lamprophyric volcanic fields [11,12]. Along the Tepic-Zacoalco rift one finds, from SE to NW: La Primavera caldera [13] Tequila volcano, Ceboruco volcano [14], San Pedro Caldera [2], Tepeltitic, Sangangüey, and Las Navajas [8]. Along the Colima rift we find the CVC [15] including El Cántaro Norte, El Cántaro Sur, Nevado de Colima, and Fuego volcanoes. The volcanic fields of Ayutla [12], Atenguillo, and Mascota [16] conform the Central Jalisco Volcanic Lineament (CJVL), a region with volcanic manifestations along 90 km [8,17,18]. San Sebastián and Los Volcanes volcanic fields are often incorporated into the CJVL; however, these volcanic fields are obviously not aligned with it. Finally, there is Tapalpa volcanic field [1,12] located about 18 km W of the Northern Colima Graben (NCG).

Two profiles with lengths ~80 km,crossing the Jalisco block with estimates of the Curie point depths were published [19]. Unfortunately, they cannot be compared with our results since the authors did not specify the locations along the profiles where the estimates were made.

A study of the Curie Isotherm (CI) covering the overall surface of Mexico is available [20]; the method we use here for the calculation of the Curie point depth is similar to the one they described in their work. However, the size of the squares ($2^o \times 2^o$ and 30' overlap) they use for their calculations is over three-times the one we use here as a reference (60×60 km^2 and 5 km overlap). The consequence is that they reach larger Curie point depths at the cost of lower spatial resolution. Our target area is smaller; the basic sampling area (60×60 km^2) allows the Curie isotherm (CI) to reach depths of 12 km-14 km,which we consider adequate to perform reconnaissance studies, and to establish relationships with the volcanic structures of the area.

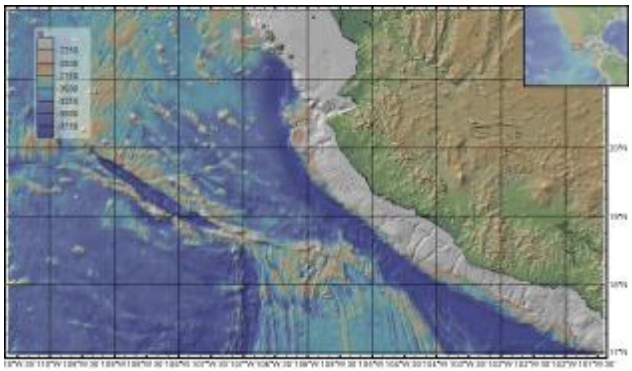

a)

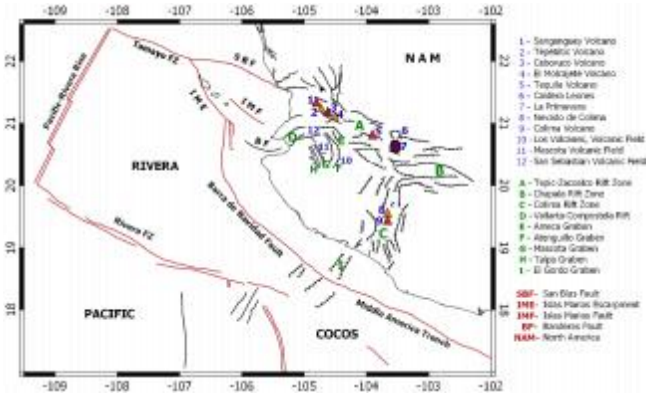

b)

Figure 1. a) Bathymetry and topography of the study area in western Mexico. b) Tectonic map of the Jalisco block and vicinity showing fault and rift systems, volcanic structures, and tectonic plates involved. Figure 1a) made with GeoMapApp (www.geomapapp.org).

2. Geology

The regional geologic map of the study area is shown in Figure 2, along with six lines in which we shall present the respective profiles (P1-P6) showing magnetic results obtained ahead.

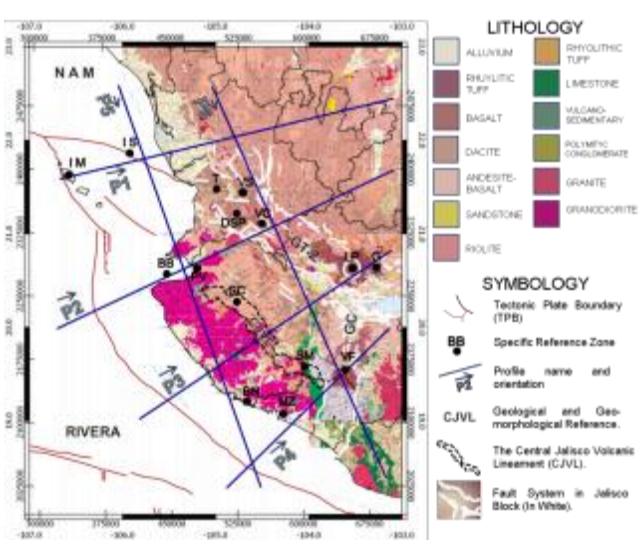

Figure 2. Regional geologic map of the study area, assembled from various maps of Servicio Geológico Mexicano [21]. Mesozoic calc-alkaline intrusive rocks (Cretaceous granites) are mostly associated with the lowlands of the Jalisco block. The region from Sierra Cacoma (SC) and Sierra Manantlán to the N and NE (i.e., the highlands above 1800 m) is mostly covered with volcanics (Early Paleogene), intermediate to mafic volcanics (6 Ma-3 Ma), and felsic volcanics (Pliocene and Quaternary). Ignimbrites from the Sierra Madre Occidental prevail in the N portion of the map. Six profiles (P1 to P6) cross the study area; they will be used to depict underground magnetic information obtained in this study.

3. Materials and Methods

3.1 Magnetic Data

Aeromagnetic data between 107° to 103W and 18° to 23N were assembled, as shown in Figure 3; it contains inland and offshore portions. Two data sources had to be combined to cover this large region: 1) data from NAMAG [22] were mainly used in the offshore region; it has a 1 km^2 cell,and it was flown at 1 km elevation. 2) for the continental area we chose data from SGM [21], with a cell size of 200 m^2 and flown at an altitude of 300 m. Both sets contain total magnetic field (TMF); consequently, it was not necessary to perform additional corrections for its use. In order not to lose resolution, the cell-size of the continental portion was maintained in the NAMAG [22] data set. Terrestrial data were upper continued 700 m to level with the altitude of NAMAG data, resulting in the map of Figure 3.

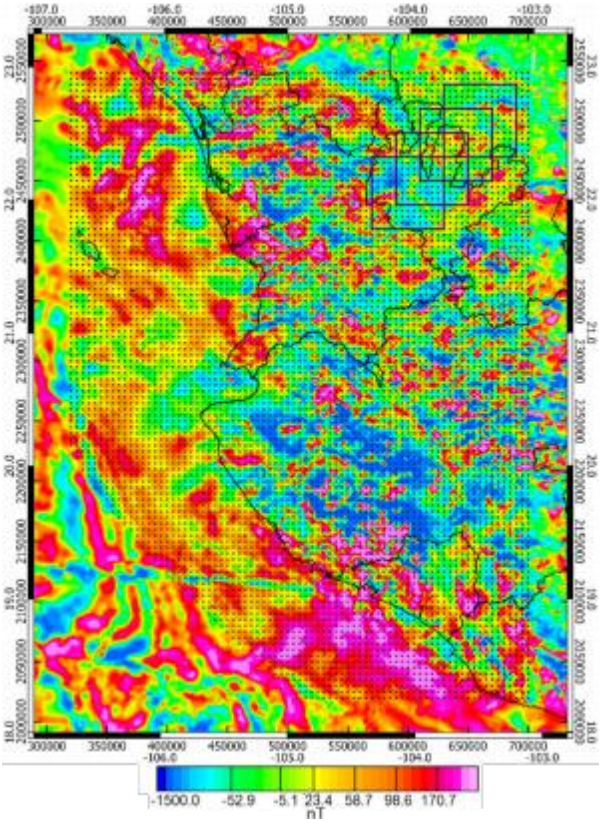

Figure 3. Map of Total Magnetic Field.

Aeromagnetic data combined from flights from NAMAG [22] and from SGM [23]. The cell size of this grid is 200 m and the flight altitude 1000 m. The equally spaced dots (7344) show the locations for which calculation of the Curie isotherm were performed in 60 × 60 km^2 areas; some examples are shown in the NE part of the figure. The offshore region reflects mainly the influence of the oceanic plates, showing the highest values of TMF. There is a drastic increment of offshore magnetic sources around the limit between the Rivera and Cocos plates [24]. The continental portion shows mostly negative magnetic values of the TMF.

3.2 Spectral Analysis

Two methods are employed for Spectral Analysis. The first statistical method [25] was proposed which relies on average tendencies and behavior of the magnetic data, allowing for estimation of the depth to the top of magnetically similar rock layers. They state that statistical mechanics postulates that power density function of irregular ensembles is equal to that of a regular ensemble averaged. Averaging of the same wavenumber is equivalent to considering that all magnetic sources are at the same depth; using the average energy amplitude of the signal implies that all sources have the same magnetic behavior.

The second methodology [26] was introduced and subsequently implemented for the analysis of highly magnetic regions and geothermal fields [27]. Finally, it was validated and defined as the Curie Isotherm Analysis [28]; it relates the magnetic susceptibility of rocks with temperature, having as a premise that in the Earth temperature increases as depth increases, as established by the geothermal gradient (25 ºC/km-30 ºC/km). Calculation of the Curie isotherm is also used to determine the maximum depth of investigation, the basement depth delineation, and the analysis of the radial power spectrum, for the regional/residual separation using filters in the wavenumber domain. The advantage of Spector & Grant's methodology [25], to be denoted Spectral Analysis, is that it is applicable to magnetic and gravity data, whilst the Curie isotherm methodology only applies to magnetic data, owing to the physical premises upon which it stands. A disadvantage of Spectral Analysis is that it yields an average result of the whole grid data set; nonetheless, it is valuable in determining regional tendencies.

3.3 The Curie Isotherm

One of the main objectives of this magnetic study consists of creating maps of the Curie Isotherm throughout the Jalisco Block (JB). A heat-flow map of Mexico is available [29] where correlation with the present results in the region of the JB show coincidences between regions of high heat-flow with shallow Curie isotherms. Of particular interest are the region surrounding Guadalajara City, where some of the highest heat-flow values are observed (>200 mW/m^2), and regions between Puerto Vallarta and Manzanillo, where this type of values has also been registered. The Curie Isotherm has also been used to constrain numerical models of some geothermal sites [30].

The Curie isotherm is the underground surface at which rock magnetization is lost; it is directly linked to the magnetic susceptibility of the rock formations and to the raise in temperature as depth increases (geothermal gradient). For the analysis of the Curie isotherm, we follow established methodology, using the spectral method to compile regional information of the magnetic anomalies [31,27]. This method is similar to a previously developed one [25] and is currently known as the Centroid Method, adding the depths to the top, to the centroid, and to the bottom of the prism generating the largest anomaly. Some constraints were established to the method [28]: the layers of the model extend to infinity horizontally, the depth to the top of the anomalous body must be less than its lateral extension, and magnetization is considered random. They use the density power spectra [32] as:

$$\varphi_{\Delta T}(k_x,k_y) = \varphi_M(k_x,k_y) \times F(k_x,k_y) \quad (1)$$

$$F(k_x,k_y) = 4\pi^2 C_m^2 |\theta_m|^2 |\theta_f|^2 e^{-2|k|Z_t}(1-e^{-|k|(Z_b-Z_t)})^2 \quad (2)$$

where:

φ_M = magnetization density power spectra

$F(k_x,k_y)$ = magnetization power spectra

k_x,k_y = Radial wave numbers in X- andY-directions

C_m = magnetic proportionality constant

θ_m = magnetization direction

θ_f = direction of the geomagnetic field

Equation (2) can be simplified observing that all its terms are radially symmetric, except $|\theta_m|^2$ and $|\theta_f|^2$; however, the radial average of these two terms is constant. If magnetization M(x,y) is random and without correlations, $\varphi_M(k_x,k_y)$ becomes constant. Thus, the average of the radial density power spectrum is:

$$\varphi_{\Delta T}(k_x,k_y) = \varphi_M(k_x,k_y)\, X\, 4\pi^2 C_m^2 |\theta_m|^2 |\theta_f|^2 e^{-2|k|Z_t} (1-e^{-|k|(Z_b-Z_t)})^2 \quad (3)$$

$$A = \varphi_M(k_x,k_y)\, X\, 4\pi^2 C_m^2 |\theta_m|^2 |\theta_f|^2) \quad (4)$$

$$\varphi_{\Delta T}(|k|) = A e^{-2|k|Z_t}\left(1-e^{-|k|(Z_b-Zt_t)}\right)^2 \quad (5)$$

For wavelengths lesser than approximately twice the layer thickness, one can apply the Napierian logarithm to Equation (5), yielding

$$- b e - \quad (6)$$

where B is a constant not dependent on depth and wavenumber, containing the sum of basic information of the media involved [27].

The depth to the top of the magnetic source can beestimated through the slope of the power spectrum of the total field.

Rewriting Equation (5) one obtains:

$$\varphi_{\Delta T}(|k|)^{\frac{1}{2}} = Ce^{-|k|Z_0}\left(e^{-|k|(Z_t-Z_0)} - e^{-|k|(Z_b-Z_0)}\right) \quad (7)$$

For very-large wavelengths this equation can be approximated as:

$$\varphi_{\Delta T}(|k|)^{\frac{1}{2}} = Ce^{-2|k|Z_0}\left(e^{-|k|(d)} - e^{-|k|(d)}\right) \approx 2|k|d * Ce^{-2|k|Z_0} \quad (8)$$

where 2d=thickness of the anomalous source.

$$\frac{\varphi_{\Delta T}(|k|)^{\frac{1}{2}}}{|k|} \approx 2d * Ce^{-2|k|Z_0} \quad (9)$$

$$Ln\left[\frac{\varphi_{\Delta T}(|k|)^{\frac{1}{2}}}{|k|}\right] = LnD - |k|Z_0 \quad (10)$$

where D is constant. An estimate of the depth of the centroid of the anomalous source can be obtained adjusting the low wavenumbers to a linear approximation of the first degree (straight line). The slope of the power spectrum is the depth of the centroid. The depth to the magnetic basement, where there are no more magnetic effects, is:

$$Z4=2Z0-Z \quad (11)$$

4. Data Processing

4.1 Spectral Aeromagnetic Analysis

A computer code was developed in Matlab using the layer model [25] for the estimate of the depths of the Curie isotherm (CI); it linearly adjusts the radial power spectra (RPS) to a given tolerance. It also assigns each result to the coordinate of the corresponding window. For the linear fit the code reads the entry data, a function was programmed that analyzes the shape of each spectrum, particularly for those required for the calculation of the CIs. The code starts reading the data with the largest amplitude and the smaller wavenumbers, up to the last datum of the power spectrum, eliminating all initial data below the maximum amplitude to guarantee a negative slope. Subsequently, the first acceptable point (P_0) is chosen, continuing up to the last point of the spectrum (P_n) and a linear inversion is performed with a first-degree function (y=mx+b) to obtain a minimum error. If the error is above the established limit, the program iterates the procedure, excluding the last point of the spectrum. The data analyzed are given by

$$\text{LnP(po:(n-i))}, \text{ where } i=0,\ 1,\ 2,\ 3,\ \ldots,\ n-3 \quad (12)$$

The process is illustrated in Figure 4.

The determination coefficient is introduced in order to evaluate whether the mathematical model adequately represents a dataset. This coefficient is the square of Pearson's correlation coefficient, that in turn measures the statistical relationship, or association, between two continuous variables, giving information about the magnitude of their association. We decided to incorporate the determination coefficient to improve the data fitting process; the program calculates simultaneously the error, the correlation coefficient, and the determination coefficient. We obtain data fitting parameters in which the error is five units or less, and the determination coefficient is > 97.5 percent. The process is applied to the spectrum of each of the data windows in which the original mesh was divided .

Maps of the layers were assembled for each of the three depths calculated: Z1 is the deepest layer, Z2 is the middle layer, and Z3 is the shallow layer. Figure 5 shows the distribution of positions for which the depths were calculated.

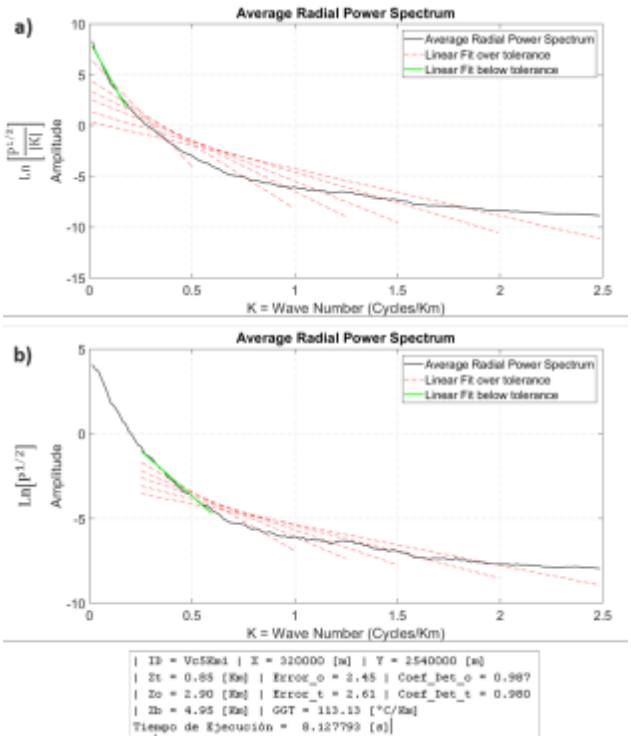

Figure 4. a) Automatic procedure to obtain the depth of the centroid of the magnetic anomalies from the original power spectrum (black), b) Estimate of the top of the magnetic anomalies from the original power spectrum (black). Red lines do not fulfill the required error and determination coefficients. ID, identification coordinates. Z_t, depth to the top. Z_0, centroid depth. Z_b; depth to the bottom.

4.2 Aeromagnetic Data Preparation

A script was prepared in Matlab for the calculation of the limits of the grid and the coordinates of the square areas. In turn, the Matlab code generated a script to be used in the Oasis Montag program, where all calculations were performed automatically. Calculation of the 7344 square areas of 60 × 60 km^2 would not have been possible without automatization of the procedure. Each selected area was extended 10 percent on every side of the square, using linear detrending and a multistep expansion method. This constitutes the mesh preparation prior to the calculations. Figure 5 exemplifies the result.

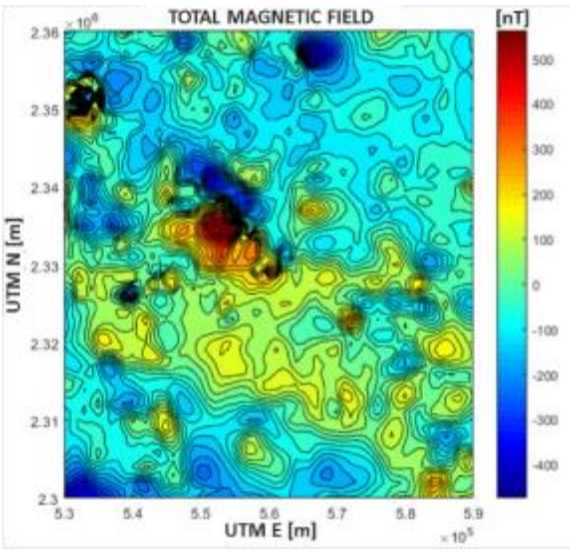

a)

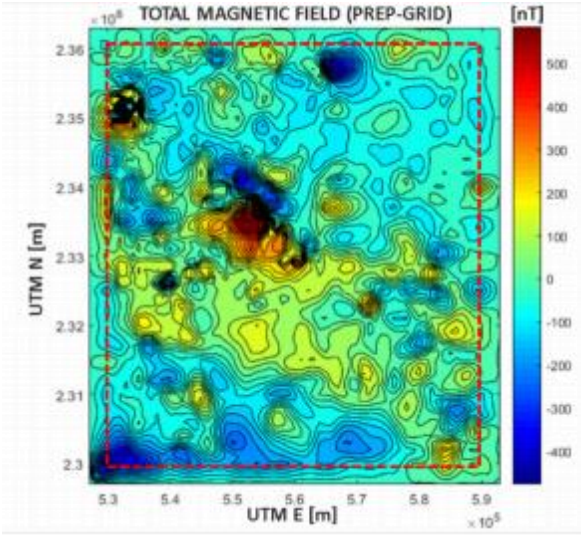

b)

Figure 5. a) original grid of the total magnetic field in a 60 × 60 km^2 area. b) the red square indicates the same area as in a), outside are the extrapolated data with a 10 percent expansion, forcing to zero the boundary values.

The 2-D Fourier transform was calculated for each window, the wavenumber distribution in rectangular coordinates was converted to polar coordinates, to finally obtain the radial power spectrum (RPS). The rest of the analytic procedure was subsequently carried out and the results were assembled in maps corresponding to the depth parameters calculated.

5. Curie Isotherms

A horizontal gradient was calculated for each map to better define the regions with the larger slope changes; this helped enclose regions with similar tendencies. Figure 6 shows the Curie isotherm map for the Jalisco block and vicinity between depths of 2.5 km and 12 km.

This map shows several regions in which the Curie isotherm shallows. Along the Tepic-Zacoalco rift two shallow regions are delimited, one associated with its SE limit, involving La Primavera caldera, and Guadalajara city; in the former some geothermal exploration is in course. The second shallow region located in the NW portion of the rift, involving Tepic city, the San Pedro dome, and Ceboruco volcano; although the CI is not as shallow as the former, in this region geothermal exploration and exploitation are already in progress. Associated to this region, the authors [5] proposed the existence of a triple point (rift, rift, rift) named the Compostela Triple Point that, together with the Guadalajara Triple Point limit the Jalisco block to the north. These two regions are separated by one in which the CI deepens, creating a singularity in the Tepic-Zacoalco rift that should be further investigated.

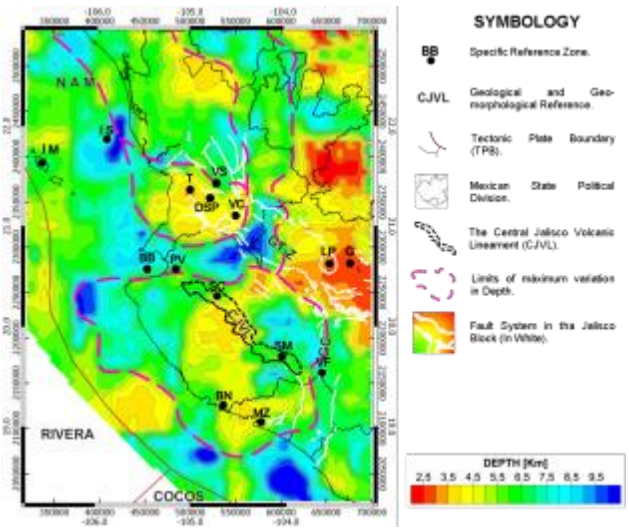

Figure 6. Map of the calculated Curie isotherm depths in the Jalisco block and its vicinity, from windows of 60 × 60 km^2 and 5 km overlap from the TMF map in Figure 3. The depths of the Curie isotherm vary from 2.5 km to 12 km. The red,dashed lines show regions delimited by high gradients in the horizontal derivative. Graben de Colima, GC; Graben de Tepic-Zacoalco, GT-Z; Islas Marías, IM; Isla Isabel, IS; Tepic City (T); Sangangüey volcano, VS; Ceboruco volcano, VC; San Pedro Lagunilla dome, DSP; La Primavera, LP; Guadalajara, G; Barra de Navidad, BN; Manzanillo, MZ; Bahía de Banderas, BB; Valle de Banderas, VB; Sierra Cacoma, SC; Sierra Manantlán, SM. Fuego (Colima) volcano, VF. North America, NAM

An unexpected result is the shallow region north of Guadalajara, affecting the states of Aguascalientes and

Jalisco; these two regions of shallow CI appear to be connected, constituting a major anomaly in the region; furthermore, they correspond to a positive Bouguer anomaly that covers practically the same region [5]. In the north portion of the map there are scattered shallow anomalies that will not be discussed, since they are quite separate from the Jalisco block.

In the central portion of the JB there is a N-S oriented anomaly, from Sierra Cacoma to Manzanillo, with CI depths between 3.5 km and 5 km. This anomaly continues southward into the offshore region, down to the Middle America Trench. Sierra Cacoma is part of the uplifted domain of the JB [6], and part of the Central Jalisco Volcanic Lineament [17]. We note the correlation between the shallow CI in the Manzanillo region and a distinctive low in the Bouguer anomaly map [5]; together they constitute an area of potential geothermal interest despite the lack of volcanic manifestations. The area between Compostela and Ceboruco volcano shows similar characteristics, a gravity low and a shallow CI; however, this region shows abundant volcanic activity.

Layer Depths

Spectral analysis is also used to calculate the surfaces of three layers that, each one, have similar average magnetic characteristics, and are useful for understanding the magnetic behavior of the crust. The selected depths for the three layers are: Z1 for the deepest layer, Z2 for the intermediate layer, and Z3 the shallowest layer. As for the CI, to better define changes in each map, as well as the regions with the larger slope changes, a horizontal gradient was calculated for each map that helps to enclose regions with similar properties. We shall now present the corresponding maps.

1) Deepest Layer

The map for the deepest layer (Z1, Figure 7), involving depths from 2.5 km to 12 km, is quite similar to that of the CI in Figure 6, owing to the similarity between the wavenumber ranges used for the depth calculation. Even the regions selected through the horizontal gradient are quite similar in both maps; they were independently calculated for each data set. However, there are differences that is convenient to note. The gradients along the Tepic-Zacoalco rift are less than those observed for the CI; the central region separating the maxima located at the extremes of the rift, although subdued, is clearly observed. This region is flanked by strong gradients, probably associated with deep crustal tectonismin that region, which differentiates the central portion of the rift from its extremes. The NW-SE region extending from Sierra Cacoma to Manzanillo appeared connected in the CI map; now it appears divided by an E-W trend, apparently isolating the Sierra Cacoma region.

2) Intermediate Layer

This layer has a depth range from 0.5 km to 2.5 km. Most of the Jalisco block appears devoid of shallow anomalies, with the exceptions noted below. The NW and SE extremes of the Tepic-Zacoalco rift remain as shallow anomalies; however, the shallowest anomalies are only present in the region N of La Primavera caldera, Sierra Cacoma, and the region around the triple point of Guadalajara. In fact, the shallow region associated with Sierra Cacoma is in the Ayutla volcanic field [12]. The anomaly around Manzanillo is more localized. Notice that the gradient limits that isolated the Tepic, San Pedro Lagunillas, Ceboruco region in the deepest layer (Z1), are now extended northwards, since the gradients are low in that direction. Towards the S the same region shows strong gradients that sharply limit its extent in that direction. The trend extends along the horizontal line from Bahía de Banderas (BB), Puerto Vallarta (PV), and up to the Tepic-Zacoalco rift (GT-Z).

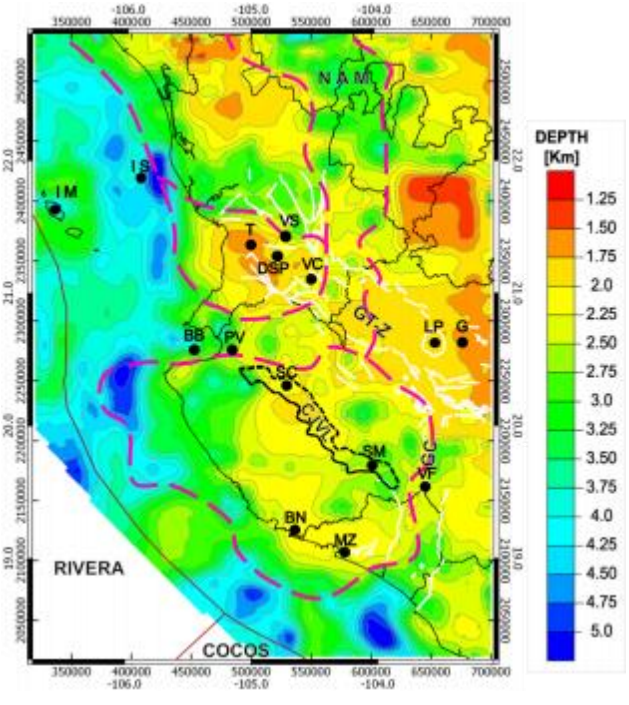

Figure 7. Map of the deepest surface (Z1) obtained with the method of Spectral Analysis, using windows of 60 × 60 km^2. Magnetic data obtained at 1000 m altitude. Depth of the surface varies from a minimum of 2.5 km to a maximum of 12 km. The horizontal derivative was calculated for this data set; the red, dashed lines show the location of high gradients, as observed for the CI. Abbreviations are as in Figure 6.

3) Surface Layer

The map of the uppermost layer is shown in Figure 9; its minimum depth is 0.2 km and its maximum depth is 1.8

km. It was obtained from the same data set as the previous maps. The map can be divided into two regions; one includes the portion north of the Jalisco block, including the offshore region, of general greater depth than the second region, encompassing most of the southern portion of the map, including the Jalisco block and the corresponding offshore region. We note that the shallow anomaly persists in the Manzanillo region, whilst that corresponding to Sierra Cacoma now appears at a greater depth.

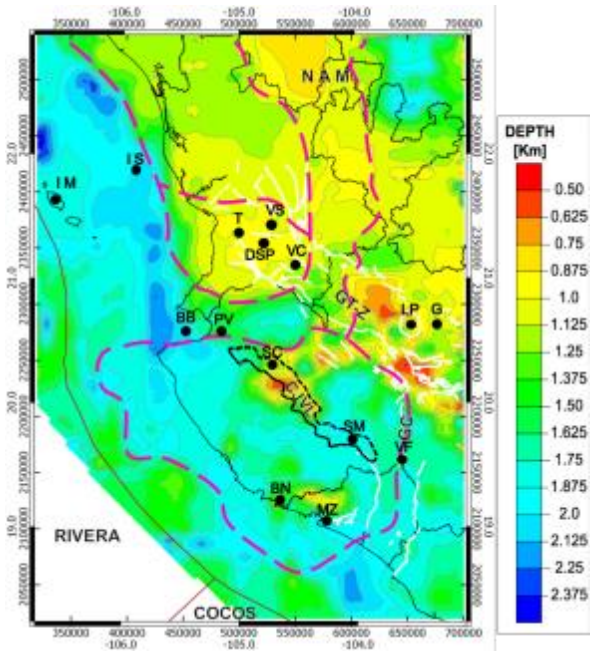

Figure 8. Map of the intermediate surface (Z2) obtained with the method of Spectral Analysis, using windows of 60 × 60 km^2. Magnetic data obtained at 1000 m altitude. Depth of the surface varies from a minimum of 0.5 km to a maximum of 2.5 km. The horizontal derivative was calculated for this data set; the red, dashed lines show the location of high gradients, as observed for the CI. The CJVL, an area close to La Primavera domes, and the SE portion of the T-Z rift, exhibit surficial anomalies in this depth range. The former two correspond to volcanic manifestations. Abbreviations and symbology are as in Figure 6.

In relation to the maps of the deep and intermediate layers (Figures 7 and 8) we see that Bahía de Banderas (BB) belongs to a limiting region, in which the bay is associated with greater layer depths that continue in a NE direction, along Valle de Banderas, the inland continuation of the graben structure of the bay [33]. In the case of the shallowest layer (Figure 9) it is even more apparent the boundary character of the bay, generally delimiting the Jalisco block and the Extensional Gulf Province [2]. These observations are inline with the proposition that Bahía de Banderas is in fact a major tectonic boundary [34].

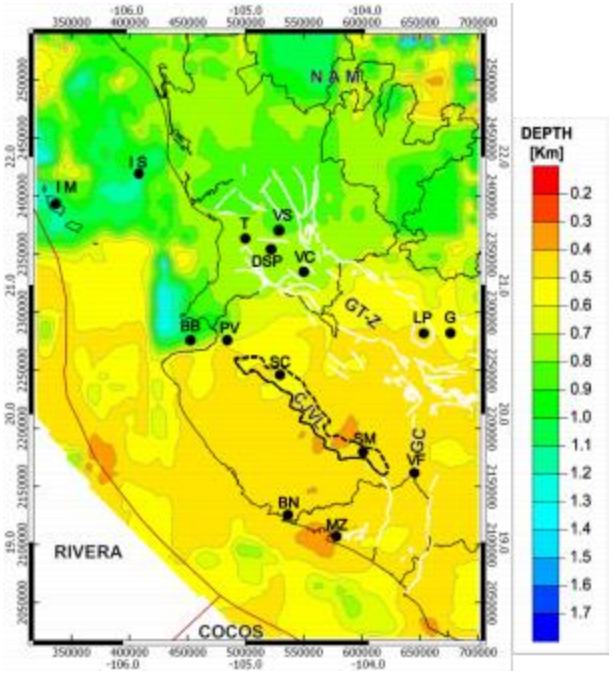

Figure 9. Map of the shallow surface (Z3) obtained with the method of Spectral Analysis, using windows of 60 × 60 km^2. Magnetic data obtained at 1000 m altitude. Depth of the surface varies from a minimum of 0.2 km to a maximum of 1.8 km. No horizontal derivative was calculated for this data set.

6. Magneto-stratigraphic Profiles

These profiles incorporate geologic, topographic, and magnetic properties along their length; location of the six profiles is shown in Figure 2. The CI map used for this interpretation is that in Figure 6, of 60 × 60 km^2.

6.1 Profile 1

This profile extends from María Madre Island (IMM) to the SW portion of Zacatecas state, close to the border with Jalisco state. It intersects three of the gradient limits shown in Figure 6, represented hereby the red, dashed rectangles. Isla Isabel (IS) is located ~ 10 km N of the line; this is a volcanic island with explosive activity [35,36]. From IMM to close to IS there is a tendency of layer Z1, and the Curie isotherm, to deepen to nearly 11 km. This layer deepening is followed by an abrupt increment to 4 km depth, coinciding with the beginning of the continental surface. From d=120 km to 340 km the depth of the CI oscillates around 6 km depth. The depth of the CI in the last portion of the profile shallows, varying between 2 km and 4 km.

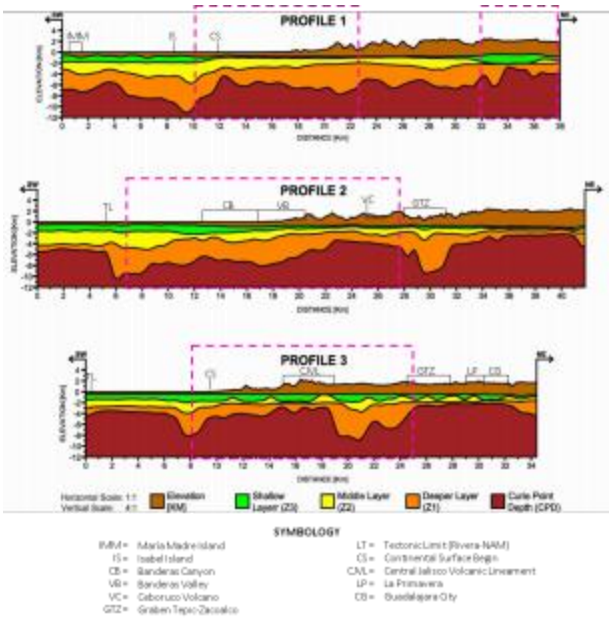

Figure 10. Graphical representation of the magnetic layers along Profiles P1, P2 and P3, shown in Figure 2,with the vertical distribution of magnetic layers Z1, Z2,and Z3 as well as the topographic profile. a) Profile 1 extends from MaríaMadre Island (IMM) to Zacatecas state. Isla Isabel, IS. Start of continental surface, SC. b) Profile 2 extends from beyond theMAT well into Aguascalientes state, crossing Bahíade Banderas (BB) and the Tepic-Zacoalco rift. c) Profile 3 extends from beyond the MATto shortly after Guadalajara city; it also crosses the Tepic-Zacoalco rift at La Primavera caldera. Invariably, the region with the strong gradients (red dashed lines) calculated with the horizontal gradient correspond to drastic drops in depth of the CI.

6.2 Profile 2

Starting SW of Bahía de Banderas, beyond the MAT, the profile crosses the Tepic-Zacoalco rift quite close to Ceboruco volcano, reaching north of Guadalajara, including the SW portion of Zacatecas state. The gradient limits are also represented hereby the red, dashed rectangles. A drastic change in depth of the CI is observed when crossing the MAT, the depth decreasing from 5 km in the oceanic platform, to 10 km in the vicinity of the trench. It is interesting to note that similar changes, not as drastic, also occur near the MAT in profiles P4, P5, and P6. The region associated with Ceboruco volcano shows shallow CI (4 km to 5 km) here and the corresponding section on Profile 6 (Figure 11); the Tepic-Zacoalco graben outstands owing to a distinct deep of the CI to depths between (9 km-11 km). It rises again in the last 100 km of the profile, including Aguascalientes state, where an anomalous region of the CI was observed (Figure 6).

6.3 Profile 3

The profile starts shortly before the MAT, the contact between the Rivera and NAM plates; it traverses Jalisco block, crosses Sierra Cacoma and La Primavera caldera, to end up slightly N of Guadalajara. A short, deep region reaching 8 km depth is located just before the continental limit is reached. Along the region designated as the static domain [6], from the coast to Sierra Cacoma, the depth of the CI oscillates around 4 km depth. As the uplifted domain is reached, the depth of the CI raises to average depths of 3 km, experiencing a drastic drop beyond the CJVL, to raise again at the SE portion of the Tepic-Zacoalco rift, La Primavera caldera and Guadalajara city. We thus observe in the continental region that shallow Curie isotherms correlate with volcanism in the surface.

6.4 Profile 4

Starting in the offshore portion of the MAT, it crosses the shoreline south of Manzanillo, quite close to the limit between the Rivera-Cocos plate boundary [24], continuing inland through the Colima Volcanic Complex (CVC) [15]. Along the offshore region the CI maintains depths of 6 km, slightly rising as approaching the continental boundary. It crosses the southern Colima graben, a region that does not show a graben [37], whose absence in that region has been attributed to the overriding of the Rivera plate by the Cocos plate [24]; here, the CI shows in that region an average depth of 5 km. Surprisingly, when reaching the vicinity of the CVC, the CI descends to depths of 6 km, rising at the end of the line in the region E of the north Colima graben (NCG) to depths of 3 km. This is the shallowest region of the CI along this line. The CI in the region corresponding to the 6-km-depth is interpreted as dominated by the structure of the NCG, which is traversed diagonally, overshadowing the influence of the eruptive materials of the CVC; however, this interpretation is speculative.

6.5 Profile 5

The profile starts NW of Isabel Island (IS); up to BB it samples the Gulf Extensional Province where two important regions are observed. The first occurs SE of IS and is one of the deepest regions found in this study for the CI, reaching 11-km-depth. The transverse profile P1 coincides in depth; not only the CI shows a deep surface but also Z2, the intermediate layer, follows that trend in both profiles. In other profiles reported herein, similar transitions in the depth of the CI are associated within the presence of the MAT. Since it is well established that this region has been extended and thinned [4], further analysis is required to elucidate the roll of this anomaly.

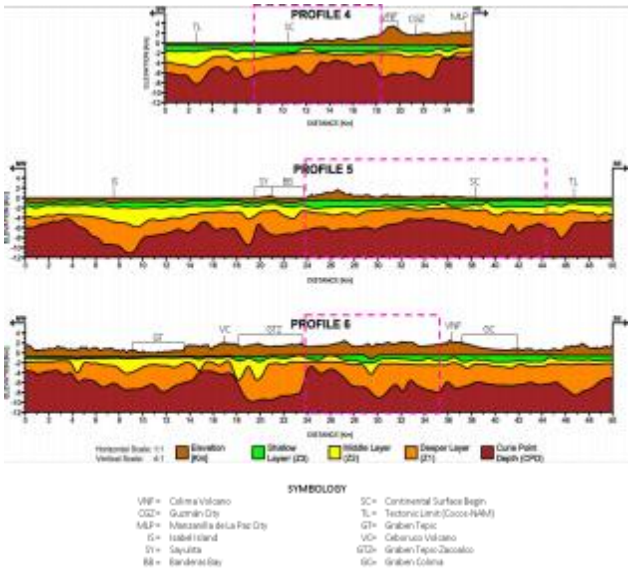

Figure 11. Graphical representation of the magnetic layers along Profiles P4, P5 and P6, shown in Figure 2, with the vertical distribution of magnetic layers Z1, Z2, and Z3 as well as the topographic profile. a) Profile 4 starts outboard of the MAT, reaches the continent penetrating south of Manzanillo, crossing the CVC and the NCG, ending south of Guadalajara and east of the NCG. b) Profile 5 starts NW, E of Isabela Island, crosses Bahía de Banderas, continues SE crossing N of Barra de Navidad (BN), ending slightly inboard of the MAT. This is the region where we observed an anomalous concentration of surficial magnetic sources (Figure 3).

According to seismic results [38], and a magnetotelluric (MT) sounding in Isabel Island [35] the depth of the subducted oceanic plate is ~24 km at that location. There is however a sharp electrical resistivity transition at ~9 km depth shown in a 1-D Bostick, and an invariant inversion [36], which could be associated with the CI deep surface.

After IS and down to the W coast of Nayarit, close to BB, the Curie isotherm rises. At the ocean-continent boundary, a rapid variation of the CI is observed, first decreasing from 6 km to 9 km, and then increasing to 5-km-depth; this rapid oscillation is also experienced by the first and second layers (Z1, Z2). An important tectonic limit has been reported in that region, where plate rollback is occurring [35]. From there, it follows the location of Bahía de Banderas; the CI experiences a continuous rise towards the SE, whilst the intermediate (Z2) and surface (Z1) layers show concave down surfaces associated with the bay. The CI rises and drops crossing the static domain of the Jalisco block, with the shallowest portion at ~5 km depth. In the vicinity of the MAT another V-shape anomaly of the CI is observed.

6.6 Profile 6

This profile is fully located in the continental region. It starts in theN of the state of Nayarit, crossing the Jalisco and Colima states, ending up in the state of Michoacán. The profile crosses a volcanic cluster (Sangangüey, San Pedro dome, and Ceboruco), the Tepic-Zacoalco rift, and the vicinity of the Colima volcano. There are two outstanding elevations of the CI, one corresponds to the region of Ceboruco volcano and the next appears immediately after crossing the Tepic-Zacoalco rift in the SE direction, where a region of silicic (6-3 Ma) and felsic (Pliocene) volcanic rocks are present. It traverses the central Colima graben, quite close to the CVC, not showing any particular behavior in this region. Layers Z1 and Z2 showslight upward deviations under the CVC; the CI shows a deep (6 km), quite short increment also at this location. The two elevated surfaces of the CI flank the region with the deepest CI along the line, which corresponds to the Tepic-Zacoalco graben. Results of Profiles 2 and 6, confirm what was already observed in Figure 6 regarding a discontinuity of the magnetic materials distribution along the rift. The Tepic-Zacoalco graben structure, contrary what would be expected, does not show continuity in these parameters. It is most likely that such discontinuity is associated with a strong tectonic alteration in that region.

6.7 3-D Representation of CI

A 3-D rendering of the Curie isotherms of the 60 × 60 km^2 map is shown in Figure 12; outstanding regions are located along Y=(2.40-2.45) × 10^6 m; the Tepic-Zacoalco graben is divided by a channel with low CI values reaching depths of 9 km to 10 km.

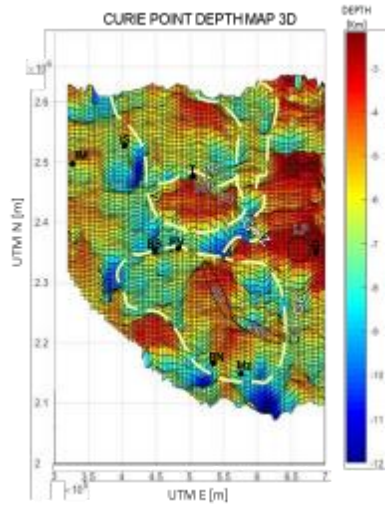

Figure 12. 3-D projection of the Curie isotherm map of the 60 × 60 km^2; Curie depths range from 2 km to 12 km. The yellow, dashed lines show the location of strong gradients, dividing the map in sectors. Abbreviations are as in Figure 6.

7. Pliocene Flare-up

The Curie isotherm maps in Figures 6 and 12 show a somewhat unexpected result along the Tepic-Zacoalco rift: the CI exhibits a strong discontinuity along the rift. With the help of the surface derivative several regions are delineated (e.g., Figure 6); these limits divide the T-Z rift into three regions: to the SE the Guadalajara-La Primavera region exhibiting shallow depths for the CI; towards the center of the rift there is a short, but neatly defined region where the CI reaches depths of over 10 km, finally follows another shallow region of the CI, at the NW portion of the T-Z rift. This evokes the structure that [2] found for the T-Z rift, namely that it is formed by various fault systems not connected to one another, with different ages and geometries. The region of deep CI invades a portion of the JB at the central portion of the rift (Figure 11, Profile 6, GTZ), then extends westward, suggesting that it may connect with BB, where the CI is not as deep.

The tectonic boundary between the Sierra Madre Occidental and the Jalisco block has been located in the T-Z rift [39,2]; however, results involving $^{40}Ar/^{39}Ar$ dates of silicic (predominantly rhyolitic) lavas and ash-flow tuffs within the Tepic-Zacoalco rift modified this view [40]. These authors dated several samples laying across the T-Z rift, reaching near the Ameca river, concluding that the southern terminus of the Sierra Madre Occidental reaches to those locations. Thus, this modified terminus abuts the Jalisco block and coincides with the region in which the CI reaches the largest depths.

Returning to the regions delineated with the surface derivatives, we note that N of the region of maximum CI depths, the lines showing the locus of large gradients are parallel for a considerable distance (e.g., Figure 7). It is also remarkable to observe that these limits coincide with Bolaños graben, a structure developed between 24 Ma-18 Ma resulting from the E-W extension experienced in western Mexico when Baja California started to separate from mainland Mexico [41]. At that time the T-Z rift had not yet developed. According to [2] two extension periods have structured the T-Z rift, one in the late Miocene (12 Ma-9 Ma), and the other in the early Pliocene (5.5 Ma-3.5 Ma), with almost no extension in the Quaternary; these authors consider that the T-Z rift represents an intraplate deformation zone that has reactivated the boundary between the Sierra Madre Occidental and the JB.

Ignimbrite flare-ups were quite common in the Sierra Madre Occidental in the 38 Ma-23 Ma period [42]. A Pliocene ignimbrite flare-up (5 Ma to 3 Ma) occurred in the T-Z rift with a minimum volume of 600 km^3 [39], attaining thicknesses of 500 m in less than 1 m.y. near Ceboruco volcano. We recall that Ferrari et al. [2] reported that a depression of 1800 m must have developed in the Ceboruco area at the beginning of late Miocene time. Pliocene basalt flows of 3.9 Ma ~ 4.0 Ma are found throughout the T-Z rift. The Pliocene basaltic lavas containing high-Ti concentrations are not typical of subduction zones; they are rather identified as ocean-island basalts. It has been considered that this type of basalt is the result of extension and decompressional melting of asthenospheric mantle, concluding that the Pliocene flare-up was a consequence of extension and lithospheric thinning [39]. Analyzing flare-ups in cordilleran arcs [42], the authors conclude that magmas associated with the flare-ups are mantle derived, attributing the cause of the flare-ups to episodic mantle processes, indicating that crustal melting is not required for triggering the flare-up.

Report of the rhyolitic flare-up is throughout the whole T-Z rift [39]; however, it is likely that the main activity center was located along the middle portion of the rift, where the Sierra Madre Occidental extension of the Bolaños graben had already weakened the region of the T-Z rift, coinciding with the present deepest location of the Curie isotherm. In the SMO, large volume ignimbritic eruptions occurred during graben collapse [41]; often, only part of the graben is involved. Since the flare-up involves the release of large quantities of heat, inducing subsequent local cooling off, of the geologic materials; we speculate that such recent, strong activity is probably the cause for the CI reaching depths >10 km in that location.

8. Areal Effect

As stated earlier, Spectral Analysis yields an average result of the area considered for the calculation, making it valuable for determining regional tendencies. Determination of the depth of the CI is related to the surface area where the magnetic field is defined for the calculation. Our intent in this section is to show how the size of the area considered for the calculation affects the result. We present the Curie Isotherm depth for areas of 30 × 30 km^2, 40 × 40 km^2, 50 × 50 km^2 and 60 × 60 km^2 with 5 km overlaps, plus 90 × 90 km2 and 120 × 120 km2 with 10 km overlaps. The overlap, or incremental distance, defines the minimum size of a genuine anomaly; that is, a true anomaly, not one caused by calculation artifacts.

In the calculation of the CI an average value of the volume considered is assigned to the corresponding central point. The regular set of central points constitutes a mesh that can be visualized in various ways; examples are the maps presented in this section. As the area increases the penetration depth increases, and the volume involved increases. Consequently, the depth of the CI will vary ac-

cording to the area involved in the estimate. Figures 13 to 15 show the results of varying the size of the calculation area of the magnetic field shown in Figure 3. The largest sampling depths are attained in the 120×120 km^2 map, reaching penetration depths of ~20 km.

This method acts as a kind of spatial filter yielding useful information on a defined depth range, where variations of the CI are associated with the magnetic properties of the sampled region. We first illustrate how the distribution of the CI changes as the size of the calculation area varies. Figure 13a shows the shallowest configuration of the CI not exceeding 6 km in depth. Red tones represent the shallowest layers of the CI. In contrast, the map in Figure 15b reaches 20 km in depth and its shallowest layers are located at 5 km depth. The information given by each map is thus only related to the layer thickness, or volume, involved.

The above figure sequence shows the distribution of the CI at various depths; it is interesting to note that there are regions in which shallow CI persists at all depth ranges involved, whilst others experience drastic changes in depth. Figure 13a shows that the central eastern portion of the map contains a region with CI depth of ~1.9 km, which is the shallowest. As the size of the area increases in Figures 13 to 15, one observes that although the CI distribution changes throughout the map, this region maintains shallow depths of the CI at all area sizes. We interpret this as a volume in which demagnetization occurs at all depths surveyed, indicating a persistent, major anomaly, implying the volume under the anomalous region contains persistent zones where rock magnetization is lost at a range of depths between 1.9 km and 7 km, and probably deeper.

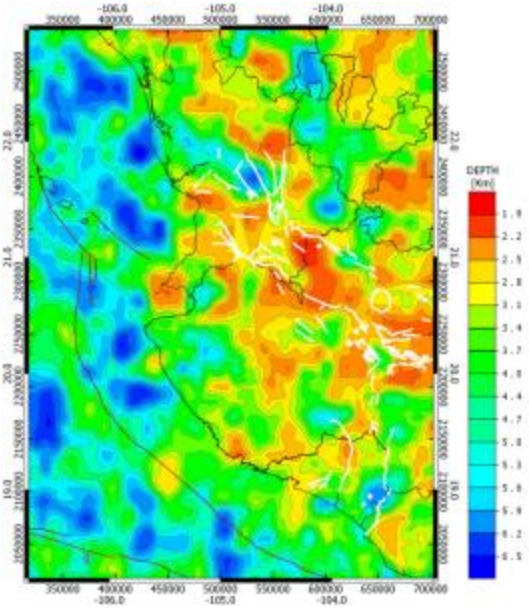

a)

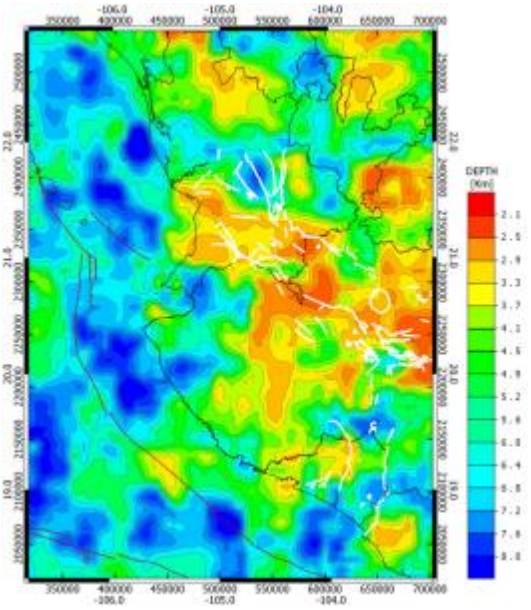

b)

Figure 13. Depth of the Curie isotherm for areas of a) 30×30 km^2 and b) 40×40 km^2 with 5 km overlap. The penetration depth increases as the area increases.

Another interesting observation involves the appearance of a shallow surface of the CI at a depth of ~4.7 km (Figure 15a) in the coastal region between Bahía de Banderas and Manzanillo, which, as the survey area is reduced, it evolves into wider regions of shallow CI (Figure 14b), reducing its size at even shallower depths (Figure 14a).

Figure 16 exemplifies the distribution of the shallow layers of the CI according to the size of the sample area. It illustrateshow the CI can be used to explore different volumes, at different depths, to draw conclusions about rock magnetization at such depths.

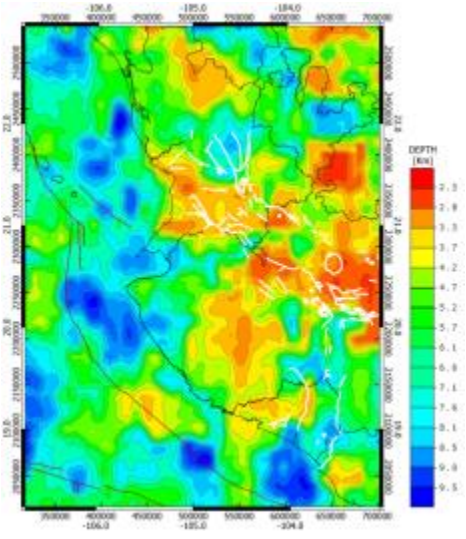

a)

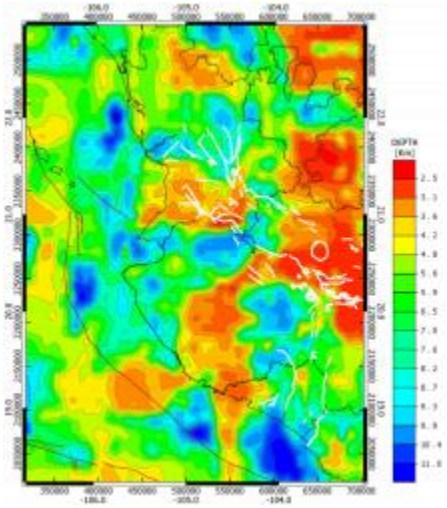

b)

Figure 14. Depth of the Curie isotherm for areas of, a) 50 × 50 km^2, and b) 60 × 60 km^2 with 5 km overlap.

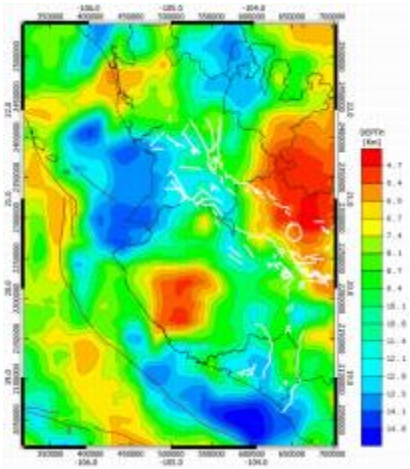

a)

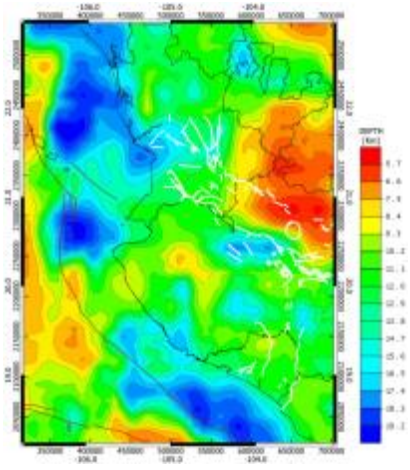

b)

Figure 15. Depth of the Curie isotherm for areas: a) 90 × 90 km^2 and b) 120 × 120 km^2 with 10 km overlap.

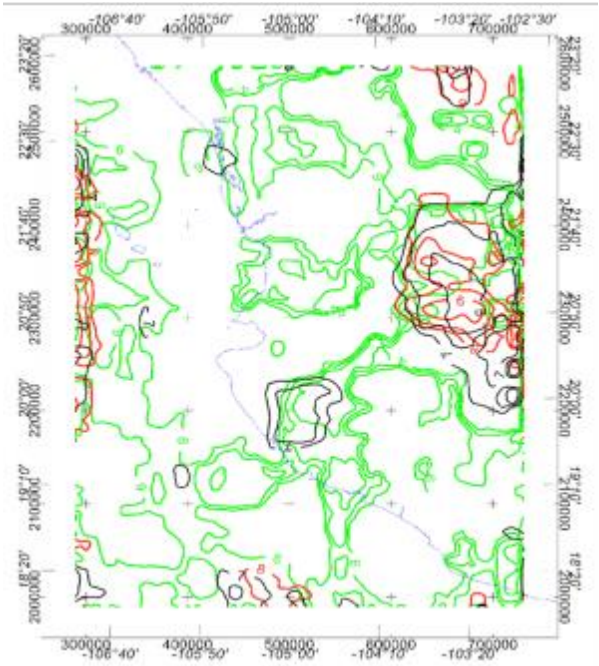

Figure 16. Depth contours of the CI corresponding to 120 × 120 (red), 90 × 90 (black), and 60 × 60 (green) km^2 areas. Persistency of the CI at different depths is only observed at the eastern portion of the map and a few peripheral fragments. Depths range from 7.5 (red) to 2.0 (green) km; Only the three shallowest contours for each distribution are plotted in each case.

9. Conclusions

Calculating the magnetization of the Earth's crust in specific regions can help understand the distribution of materials associated with this physical property in the upper surfaces of the crust; the observed magnetic field is the input parameter for the calculations. The Curie Isotherm can be obtained by means of Spectral Analysis, which yields results according to the size of the sample area. Generally speaking, we observe that volcanic regions in the Jalisco block are usually associated with shallow Curie isotherms, although not all shallow CI correspond with volcanic regions. This regional study will be an element for comparison with local results in the Jalisco block; comparison with gravimetric, seismic and geothermal studies in particular areas of interest is feasible.

An unexpected result regarding the behavior of the Curie isotherm was obtained along the Tepic-Zacoalco rift, southeast of Ceboruco volcano. The CI changes from depths of 4 km~5 km to depths of 9 km~10 km in a short distance and then rises again to the former depths. The rift is a NW-SE alignment of grabens and half-grabens with numerous volcanic structures along its length, implying

that numerous heat sources are emplaced there. Finding a comparatively cold region, where the CI reaches depths of 9 km~10 km in a portion of the rift, constitutes an anomaly. This anomaly appears from the 50 × 50 km^2 to the 90 × 90 km^2 maps of the CI, delimiting its depth from 5 km to 13 km. We tentatively associated this CI anomaly with the Pliocene ignimbrite flare-up registered in the T-Z rift with a minimum volume of 600 km^3 [39]. From the CI maps we estimate a minimum area of 100 km^2 and an average thickness of 7 km, yielding a minimum volume of 700 km^3, inline with the geological estimate given above.

Analyzing the behavior of magnetization as a function of the area used for the calculation, one can determine how de-magnetization evolves as a function of depth. From these results one can observe how deep CI regions of limited size appear to evolve into wider, surficial, less intensely demagnetized regions. In any Curie depth calculation, one must bear in mind the dependence of its value from the averaged value of the area assigned to that point. The discussion on the areal effect on the calculation of the Curie isotherm has been substantiated with extensive calculations that allowed to draw the mentioned conclusions.

When we compare the Bouguer anomaly calculated in the whole Jalisco block [5] with regions in which the CI shows a persistent presence at depths varying from 2 km to 8 km, a good correlation is observed with the two major gravimetric anomalies reported in the Jalisco block. To explain this correlation, one must have in these crustal volumes the presence of denser rocks, as well as a region of higher temperatures. It appears feasible that in such volumes, crustal layers have been altered by uprising asthenospheric materials, with larger rock densities and temperatures higher than those corresponding to the geothermal gradient, inducing the gravity and temperature anomalies associated with these observations. These preliminary arguments should be corroborated in future studies.

Conflict of Interest

There is no conflict of interest.

Acknowledgments

This study has been supported by Facultad de Ingeniería, UNAM and IIMAS, UNAM; we acknowledge material support from both institutions. This research did not receive any specific grant from funding agencies in the public, commercial, or not-for-profit sectors.

References

[1] Allan, J.F., 1986. Geology of the Colima and Zacoalco grabens, SW Mexico: Late Cenozoic rifting in the Mexican Volcanic Belt. Geological Society of America Bulletin. 97, 473-485.

[2] Ferrari, L., Rosas-Elguera, J., 1999. Late Miocene to Quaternary extension at the northern boundary of the Jalisco block, western Mexico: The Tepic-Zacoalco rift revised. *in* Delgado-Granados, H., Aguirre-Díaz, G., and Stock, J. M., eds., Cenozoic Tectonics and Volcanism of Mexico: Boulder, Colorado. Geological Society of America. Special Paper. pp. 334.

[3] Duque-Trujillo, J., Ferrari, L., Orozco-Esquivel, T., et al., 2015. Timing of rifting in the Southern Gulf of California and its conjugate margins: Insights from the plutonic record. Geological Society of America Bulletin. 127(5-6), 702-736.
DOI: https://doi.org/10.1130/B31008.1

[4] Ferrari, L., Orozco-Esquivel, T., Bryan, S.E., et al., 2018. Cenozoic magmatism and extension in western Mexico: Linking the Sierra Madre Occidental silicic large igneous province and the Comondú Group with the Gulf of California rift. Earth Science Reviews. 183, 115-152.
DOI: https://doi.org/10.1016/j-earscirev.2017.04.006

[5] Camacho, M., Alvarez, R., 2020. Gravimetric analysis of the rifts and volcanic fields of the Jalisco block, Mexico. Tectonophysics. 791, 228577.
DOI: https://doi.org/10.1016/j.tecto.2020.228577

[6] Alvarez, R., López-Loera, H., Arzate, J., 2006. Evidence of the existence of an uplifted and a static domain in the Jalisco Block. In: Backbone of the Americas: Patagonia to Alaska, Mendoza, Argentina: Geological Society of America. Abstracts with Programs, Specialty Meetings. 2, 108.

[7] Cassel, E.J., Smith, M.E., Jicha, B.R., 2018. The impact of slab rollback on Earth's surface: Uplift and extension in the hinterland of the North American Cordillera. Geophysical Research Letters. 45(10), 996-11,004.
DOI: https://doi.org/10.1029/2018GL079887

[8] Gómez-Tuena, A., Langmuir, C.H., Goldstein, S.L., et al., 2007. Geochemical evidence for slab melting in the Transmexican Volcanic Belt. Journal of Petrology. 48, 537-562.
DOI: https://doi.org/10.1093/petrology/egl071

[9] Rosas-Elguera, J.L., Ferrari, L., Garduño-Monroy, V., et al., 1996. Continental boundaries of the Jalisco block in the Pliocene-Quaternary kinematics of western Mexico. Geology. 24, 924.

[10] Gastil, G., Krumenacher, D., Jensky, W.A., 1978. Reconnaissance geology of west central Nayarit, Mexico. Geological Society of America Bulletin. 90, 839-857.

[11] Lange, R.A., Charmicael, I.S.E., 1991. A potassic volcanic front in western Mexico: Manifestations of an incipient eastward spreading ridge jump. Geology. 13, 54-57.

[12] Righter, K., Rosas-Elguera, J., 2001. Alkaline lavas in the volcanic front of the western Mexican Volcanic Belt: Geology and petrology of the Ayutla and Tapalpa volcanic fields. Journal of Petrology. 42(12), 2333-2361.

[13] Mahood, G.A., Drake, R.E., 1982. K-Ar dating young rhyolitic rocks: A case study of the Sierra La Primavera, Jalisco, Mexico. Geological Society of America Bulletin. 93, 1232-1241.
DOI: https://doi.org/10.1130/0016-7606(1982)93<1232:K-DYRRA>2.0.CO;2

[14] Rodríguez Uribe, M.C., Núñez-Cornú, F.J., Nava Pichardo, F.A., et al., 2013. Some insights about the activity of the Ceboruco Volcano (Nayarit, Mexico) from recent seismic low-frequency activity. Bulletin of Volcanology. 75, 755.
DOI: https://doi.org/10.1007/s00445-013-0755-9

[15] Luhr, J.F., Carmichael, I.S.E., 1980. The Colima Volcanic Complex, Mexico. Contributions to Mineralogy and Petrology. 71, 343-372.

[16] Ownby, S.E., Lange, R.A., Hall, C.M., 2008. The eruptive history of the Mascota volcanic field, western Mexico: Age and volume constraints on the origin of andesite among a diverse suite of lamprophyric and calc-alkaline lavas. Journal of Volcanology and Geothermal Research. 177(4), 1077-1091.
DOI: https://doi.org/10.1016/j.jvolgeores.2008.08.002

[17] Bandy, W.L., Urrutia-Fucugauchi, J., McDowell, F.W., et al., 2001. K-Ar ages of four mafic lavas from the Central Jalisco Volcanic Lineament: Supporting evidence for a NW migration of volcanism within the Jalisco block, western Mexico. Geofisica Internacional. 40, 259-269.

[18] Suhardja, S.K., Grand, S.P., Wilson, D., et al., 2015. Crust and subduction zone structure of Southwestern Mexico. Journal of Geophysical Research. Solid Earth. 120, 1020-1035.
DOI: https://doi.org/10.1002/2014JB011573

[19] Campos-Enríquez, J.O., Arroyo-Esquivel, M.A., Urrutia-Fucugauchi, J., 1990. Basement, Curie isotherm and shallow crustal structure of the Trans-Mexican Volcanic Belt, from aeromagnetic data. Tectonophysics. 172, 77-90.

[20] Manea, M., Manea, V.C., 2011. Curie Point Depth Estimates and Correlation with Subduction in Mexico. Pure & Applied Geophysics. 168, 1489-1499.
DOI: https://doi.org/10.1007/s00024-010-0238-2

[21] SGM (Servicio Geológico Mexicano), 1997. Geological-Mining Charts: F13-6, F13-8, F13-9, F13-3, F13-5, F13-11, F13-2-5, F13-12,and F13-6-9.

[22] NAMAG (North American Magnetic Anomaly Group), 2002. Magnetic Anomaly Map of North America. US Department of the Interior and US Geological Survey. Map, scale 1:10,000,000.

[23] SGM (Servicio Geológico Mexicano), 1983. Magnetic Anomaly Map of Jalisco Block.

[24] Alvarez, R., Yutsis, V., 2015. The elusive Rivera-Cocos plate boundary: not diffuse.From: Wright, T.J., Ayele, A., Ferguson, D.J., Kidane, T. & Vye-Brown, C. (eds) Magmatic Rifting and Active Volcanism. Geological Society, London, Special Publications. pp. 420.
DOI: http://doi.org/10.1144/SP420.8

[25] Spector, A., Grant, F.S., 1970. Statistical models for interpreting aeromagnetic data. Geophysics. 35(2), 293-302.

[26] Bhattacharyya, B.K., Leu, L., 1975. Spectral Analysis of gravity and magnetic anomalies due to two-dimensional structures. Geophysics. 40(6), 993-1013.

[27] Okubo, Y., Graf, R.J., Hansen, R.O., et al., 1985. Curie point depths of the island of Kyushu and surrounding areas, Japan. Geophysics. (53-3), 81-94.

[28] Tanaka, A., Okubo, Y., Matsubayashi, O., 1999. Curie point depth based on spectrum analysis of the magnetic anomaly data in East and Southeast Asia. Tectonophysics. 306, 461-470.

[29] Prol-Ledesma, R.M., Carrillo-dela Cruz, J.L., Torres-Vera, M.A., et al., 2018. Heat flow map and geothermal resources in Mexico. Terra Digitalis. 2(2), 1-15.

[30] Guerrero-Martínez, F.J., Prol-Ledesma, R.M., Carrillo-dela Cruz, J.L., et al., 2020. A three-dimensional temperature model of the Acoculco caldera complex, Puebla, Mexico, from the Curie isotherm as a boundary condition. Geothermics. 86, 101794.
DOI: https://doi.org/10.1016/j.geothermics.2019.101794

[31] Shuey, R.T., Schellinger, D.K., Tripp, A.C., et al., 1977. Curie depth determination from aeromagnetic spectra. Geophysical Journal of the Royal Astronomical Society. 50(1), 75-101.

[32] Blakely, R.J., 1996. Potential theory in gravity and magnetic applications. London, England. Cambridge University Press.

[33] Alvarez, R., 2002. Banderas Rift Zone: A Plausible NW Limit of the Jalisco Block. Geophysical Research Letters. 29(20), 1994-1997.
DOI: https://doi.org/10.1029/2002GL016089

[34] Alvarez, R., Corbo-Camargo, F., Yutsis, V., 2021.

The great tectonic discontinuity of Bahía de Banderas, Mexico. Tectonophysics. 803, 228762. DOI: https://doi.org/10.1016/j.tecto.2021.228762

[35] Alvarez, R., Corbo-Camargo, F., Yutsis, V., 2017. Geophysical modelling of Isla Isabel: a volcanic island on the Mexican continental margin. From: Németh, K., Carrasco-Núñez, G., Aranda-Gómez, J.J. & Smith, I.E.M. (eds) Monogenetic Volcanism. Geological Society, London, Special Publications. pp. 446. DOI: https://doi.org/10.1144/SP446.13

[36] Alvarez, R., Corbo-Camargo, F., Yutsis, V., et al., 2017. A volcanic centre in Mexico's Pacific continental shelf. From: Németh, K., Carrasco-Núñez, G., Aranda-Gómez, J. J. & Smith, I. E. M. (eds) Monogenetic Volcanism. Geological Society, London, Special Publications. pp. 446. DOI: https://doi.org/10.1144/SP446.12

[37] Serpa, L., Smith, S., Katz, C., et al., 1992. A geophysical investigation of the southern Jalisco block in the State of Colima, Mexico. Geofisica Internacional. 31, 475-492.

[38] Lizarralde, D., Axen, G.J., Brown, H.E., et al., 2007. Variable styles of rifting in the Gulf of California. Nature. 448, 466-469.

[39] Frey, H.M., Lange, R.A., Hall, C.M., et al., 2007. A Pliocene ignimbrite flare-up along the Tepic-Zacoalco rift: Evidence for the initial stages of rifting between the Jalisco block (Mexico) and North America. GSA Bulletin. 119(1/2), 49-64. DOI: https://doi.org/10.1130/B25950.1

[40] Ferrari, L., López-Martínez, M., Orozco-Esquivel, M.T., et al., 2013. Late Oligocene to middle Miocene rifting and syn-extensional magmatismin the southwestern Sierra Madre Occidental, Mexico: The beginning of the Gulf of California rift. Geosphere. 9(5), 1161-1200.

[41] Aguirre-Díaz, G.J., Labarthe-Hernández, G., Tristán-González, M., et al., 2008. The ignimbrite flare-up and graben calderas of the Sierra Madre Occidental. Developments in Volcanology. DOI: https://doi.org/10.1016/S1871-644X(07)00004-6

[42] Martínez Ardila,A.M., Paterson, S.R., Memeti, V., et al., 2019. Mantle driven Cretaceous flare-ups in cordilleran arcs. Lithos. (326-327), 19-27.